Ocean Systems Engineering, *Vol. 3, No. 4 (2013) 327-348*
DOI: http://dx.doi.org/10.12989/ose.2013.3.4.327

Energy extraction from the motion of an oscillating water column

Hao Wang and Jeffrey M. Falzarano*

Ocean Engineering Program, Texas A&M University, College Station, Texas, USA

(Received November 25, 2013, Revised November 27, 2013, Accepted December 8, 2013)

Abstract. An Oscillating Water Column (OWC) is a relatively practical and convenient device that converts wave energy to a usable form, which is electricity. The OWC is kept inside a fixed truncated vertical cylinder, which is a hollow structure with one open end submerged in the water and with an air turbine at the top. This research adopts potential theory and Galerkin methods to solve the fluid motion inside the OWC. Using an air-water interaction model, OWC design for energy extraction from regular wave is also explored. The hydrodynamic coefficients of the scattering and radiation potentials are solved for using the Galerkin approximation. The numerical results for the free surface elevation have been verified by a series of experiments conducted in the University of New Orleans towing tank. The effect of varying geometric parameters on the response amplitude operator (RAO) of the OWC is studied and modification of the equation for evaluating the natural frequency of the OWC is made. Using the model of air-water interaction under certain wave parameters and OWC geometric parameters, a computer program is developed to calculate the energy output from the system.

Keywords: oscillating water column; Galerkin approximation; natural frequency; wave height; turbine constant; truncated vertical cylinder

1. Introduction

For over a half century, the increasing world-wide demand for energy has been driving scientists and engineers into finding new energy resources. Wave energy is viewed as a promising renewable energy resource and more than 150 wave energy extraction device concepts have been created, including attenuator, point absorber, overtopping device and other new technologies (Falzarano *et al*. 2012).

Among the wave energy conversion devices, the Oscillating Water Column (OWC) device is a fixed cylinder with air flow output from it driven by the oscillating wave elevation inside the device. Usually an air turbine is installed with a generator to convert the motion of the air flow into electricity. Garrett (1970) was the first to study the progressive wave induced fluid motion inside a hollow cylinder partially immerged in finite water depth. Sarmento and Falcão (1985) did a two-dimensional analysis of an OWC device using linear wave theory. Malmo and Reitan (1985) conducted calculations of the wave power absorption by a squared oscillating water column in a channel. Linton and Evans (1992) studied the wave scattering and radiation by a vertical circular cylinder placed on a channel using the multipole method. Evans and Porter (1995, 1997) came up

*Corresponding author, Professor, E-mail: jfalzarano@civil.tamu.edu

http://www.techno-press.org/?journal=ose&subpage=7 ISSN: 2093-6702 (Print), 2093-677X (Online)

with accurate and efficient numerical method to solve for the OWC hydrodynamic coefficients using the Galerkin method. Falnes (2002) developed a theoretical model for the OWC device with a pneumatic power takeoff. Cho (2002) studied the energy output from a circular cylinder using a real-valued turbine constant. Garriga and Falzarano (2008) calculated the water surface elevation using existing potential theory and compared it with the experimental result from the UNO towing tank. Koo and Kim (2010, 2012) conducted a time-domain simulation of land-based Oscillating Water Column using nonlinear model with viscous damping, and they used OWC model to estimate the performance of a European wave power plant as well to simulate different configurations. Using either a numerical or experimental method, researchers such as Gato and Falcão (1988), Camporeale *et al*. (2011) conducted studies of the Wells turbine, which is widely used for OWC device power takeoff.

The purpose of this research is to combine the existing potential theory for the scattering and the radiation problem for a truncated vertical cylinder with the model for the interaction between water surfaces and air flow through a turbine. This combination result in a complete program to analyze and optimize the OWC device design. In order to show a complete theoretical background of the numerical model, the authors follow the derivation procedure by Evans and Porter (1997).

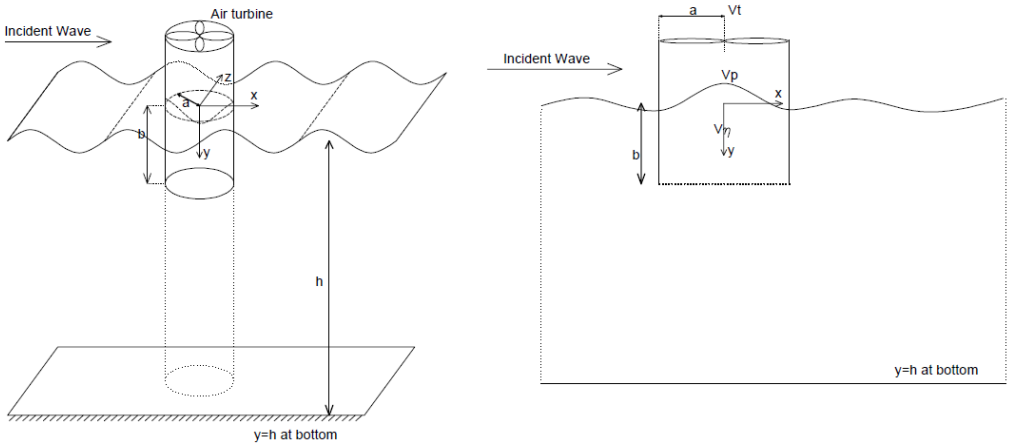

Fig. 1 Concept of the OWC device

2. Mathematical model

Fig. 1 shows the OWC system concept, where a is the radius of the cylinder, *b* is the draft of the cylinder, and *h* is the water depth.

The following subsection combines Evans and Porter's (1997), Garriga and Falzarano's (2008) and Wang's (2013) derivation to solve for the wave potential.

We assume a harmonic wave with time dependence $e^{-i\omega t}$. $The\ variable\ \omega$ is the angular frequency of the incident wave. The pressure oscillation and wave elevation have the same frequency because of linearity, so

$$\Phi(x,y,z) = Re\{\phi(x,y,z)e^{-i\omega t}\} \tag{1}$$

$$\eta(x,z,t) = Re\{\eta(x,z)e^{-i\omega t}\} \tag{2}$$

$$p_e = Re\{pe^{-i\omega t}\} \tag{3}$$

$P(t) = p_a + p_e$, P(t) is the air pressure about the free surface, p_a is the atmosphere air pressure, p_e is the oscillating part of the air pressure. η is the surface elevation and wave height H=2η for regular wave. We can remove the time dependence of the fluid potential to deal with the time-independent potential, denoted by ϕ.

$$\frac{\partial\phi}{\partial y}|_{(y=0)} + \frac{\omega^2}{g}\phi|_{(y=0)} = \begin{cases} -\frac{i\omega}{\rho g}p, & \text{Inside the cylinder} \\ 0, & \text{Outside the cylinder} \end{cases} \tag{4}$$

According to Evans (1982), the time-independent potential can be decomposed into two parts

$$\phi = \phi^S - \frac{i\omega p}{\rho g}\phi^R \tag{5}$$

In which ϕ^S is the scattering potential,ϕ^R is the radiation potential related to the radiated waves due to oscillating air pressure on the water surface inside the cylinder. According to Evans and Porter (1997), apply the radiation potential to Eq. (4). Inside the cylinder

$$\frac{\partial\phi^R}{\partial y}|_{y=0} + \frac{\omega^2}{g}\phi^R|_{y=0} = \begin{cases} 1, & \text{Inside the cylinder} \\ 0, & \text{Outside the cylinder} \end{cases} \tag{6}$$

Since the scattering potential is separated from the air pressure related term, the linear combined free-surface boundary condition for scattering potential is

$$\frac{\partial\phi^S}{\partial y}|_{y=0} + \frac{\omega^2}{g}\phi^S|_{y=0} = 0 \tag{7}$$

It is more convenient to express the wave potential in cylindrical coordinate system(r,θ,y).The Laplace equation in cylindrical coordinates is

$$\frac{1}{r}\frac{\partial}{\partial r}\left(r\frac{\partial\phi}{\partial r}\right) + \frac{1}{r^2}\frac{\partial^2\phi}{\partial\theta^2} + \frac{\partial^2\phi}{\partial y^2} = 0 \tag{8}$$

The potential can be solved using separation of variable

$$\phi(r,\theta,y) = \varphi_i(r,\theta)\psi_i(y) \tag{9}$$

By separation of variables, we can achieve the general form of solution to the Laplace equation as an eigenfunction expansion

$$\frac{1}{\varphi_i}\frac{1}{r}\frac{\partial}{\partial r}\left(r\frac{\partial\varphi_i}{\partial r}\right) + \frac{1}{\varphi_i}\frac{1}{r^2}\frac{\partial^2\varphi_i}{\partial\theta^2} = {k_i}^2 \tag{10}$$

$$\frac{1}{\psi_i}\frac{\partial^2\psi_i}{\partial y^2} = -{k_i}^2 \tag{11}$$

The boundary condition for ψ_i is

$$\frac{\partial\psi_i}{\partial y}|_{y=h} = 0 \tag{12}$$

$$\frac{\partial\psi_i}{\partial y}|_{y=0} + \frac{\omega^2}{g}\psi_i|_{y=0} = 0 \tag{13}$$

The remaining part in this subsection is given following solutions of partial differential equation by Haberman (2004).

According to typical solution to ordinary differential equation

$$\psi_i = a_1 cos[k_i(h-y)] + a_2 sin[k_i(h-y)] \tag{14}$$

$$\frac{\partial\psi_i}{\partial y}|_{y=h} = -a_2 k_i = 0 \tag{15}$$

When k_i=0, all solutions will be trivial. So a_2=0.

$$\psi_i = a_1 cos[k_i(h-y)] \tag{16}$$

Apply the linearized free surface boundary condition

$$\frac{\partial\psi_i}{\partial y}|_{y=0} + \frac{\omega^2}{g}\psi_i|_{y=0} = k_i A sin(k_i h) + A\frac{\omega^2}{g}cos\,(k_i h) = 0 \tag{17}$$

So k_i satisfies

$$\frac{\omega^2}{g} + k_i\, tan(k_i h) = 0 \tag{18}$$

The equation can also have an imaginary solution. When $k_0 = ik$, k is the wave number for progressive wave.

$$\psi_0 = a_1 cosh[k(h-y)] \tag{19}$$

According to

$$cosh(x) = cos(ix)\,, tan\,h(x) = -i\cdot tan(ix) \tag{20}$$

The progressive wave dispersion relationship is

$$\frac{\omega^2}{g} = k\, tanh(kh) \tag{21}$$

We can use the orthogonal identity of the eigenfunction to solve for a_1. If we write $\varphi_i(r,\theta) = f(r)g(\theta)$, we get

$$\frac{1}{f}\frac{1}{r}\frac{d}{dr}\left(r\frac{df}{dr}\right)+\frac{1}{g}\frac{1}{r^2}\frac{d^2g}{d\theta^2}={k_i}^2 \tag{22}$$

Multiplying both sides with $r^2$and separating the two eigenfunctions

$$-\frac{1}{g}\frac{d^2g}{d\theta^2}=\mu \tag{23}$$

$$r\frac{d}{dr}\left(r\frac{df}{dr}\right)+\left(-{k_i}^2r^2-\mu\right)f=0 \tag{24}$$

According to the symmetry of the flow around the cylinder, at $\theta=0$, the tangential velocity must be zero

$$\frac{dg}{d\theta}(0)=0 \tag{25}$$

According to the solution of the ordinary differential equation

$$g(\theta)=b_1\cos(q\theta)+b_2\sin(q\theta) \tag{26}$$

So $b_2=0$.

$$g(\theta)=b_1\cos(q\theta) \tag{27}$$

When $-{k_i}^2>0$, only one wave number $k_0=k$ suitable for the solution. So

$$f(r)=c_1H_q^{(1)}(kr)+c_2H_q^{(2)}(kr),\qquad where\ \mu=q^2 \tag{28}$$

When ${k_i}^2>0$, there are wave numbers k_i for the solution. This is the standing wave eigenfunction in radial coordinates

$$f(r)=c_3I_q(k_ir)+c_4K_q(k_ir),\qquad where\ \mu=q^2 \tag{29}$$

$H_q^{(1)}\ and\ H_q^{(2)}$ represent the Hankel function of first and second kind respectively (with the order of q); $I_q\ and\ K_q$ represent the modified Bessel function of first and second kind respectively (with the order of q); J_q is the original Bessel function(with the order of q).

This section gives the general form of the eigenfunction expansion for the wave potential. In the following section when we are solving the scattering and radiation problem, we will adopt the form above.

3. Motion calculation of the oscillating water column

3.1 Hydrodynamic coefficients in scattering problem

The scattering problem is induced by the incident wave when there is no radiation. For a progressive wave that travels in the positive x direction, Chakrabarti (1987) gives the time-independent incident wave potential as

$$\phi^I = \sum_{q=0}^{\infty} \epsilon_q \, i^q J_q(kr)\cos(q\theta)\psi_0(y)\,, where\ \epsilon_0 = 1, \epsilon_q = 2, for\ q \geq 1 \tag{30}$$

The derivation in this subsection was given by Evans and Porter (1997).

The scattering potential in a cylindrical coordinate system is ϕ^S.Outside the cylinder ($r \geq a$)

$$\phi^S = \sum_{q=0}^{\infty} \epsilon_q \, i^q \, cos(q\theta) \left[\left(J_q(kr) + \alpha_{q,0}^S H_q(kr) \right) \psi_0(y) + \sum_{i=1}^{\infty} \alpha_{q,i}^S \, K_q(k_i r)\psi_i(y) \right] \tag{31}$$

The first term represents the incident waves; the second term is associated with $\alpha_{q,0}^S H_q(kr)$ and is the outgoing progressive waves, and the last term with $\alpha_{q,i}^S K_q(k_i r)$ is the wave modes which are exponentially decaying.

Inside the cylinder ($r \leq a$)

$$\phi^S = \sum_{q=0}^{\infty} \epsilon_q \, i^q \cos(q\theta) \left[\beta_{q,0}^S J_q(kr)\psi_0(y) + \sum_{i=1}^{\infty} \beta_{q,i}^S \, I_q(k_i r)\psi_i(y) \right] \tag{32}$$

The first term is associated with $\beta_{q,0}^S$ is the standing wave modes inside the cylinder, and the $\beta_{q,i}^S$ terms are the exponentially decaying disturbances. $\psi_0(y)$ and $\psi_i(y)$ are the eigenfunctions in the y direction, if we write

$$\psi_0(y) = \frac{1}{M_0}\cosh k(h-y), \text{ where } M_0 = \sqrt{\frac{1}{2}\left(1 + \frac{sinh2kh}{2kh}\right)} \tag{33}$$

$$\psi_i(y) = \frac{1}{M_i}\cos k_i(h-y), where\ M_i = \sqrt{\frac{1}{2}(1 + \frac{sin2k_i h}{2k_i h})}\,, i \geq 1 \tag{34}$$

The variables $k\ and\ k_i$ are the wave numbers which satisfy the dispersion relation given in the previous section. If we write

$$\frac{\partial \phi^S}{\partial r}|_{r=a} = \sum_{q=0}^{\infty} \epsilon_q \, i^q \cos(q\theta)\, U_q^S(y) \tag{35}$$

$U_q^S(y)$ is the radial velocity at the radius of the cylinder with mode q. The radial velocity at the radius of the cylinder should be consistent whether we calculate it according to the potential expression outside the cylinder or inside the cylinder. In addition, both inside and outside of the cylinder belong to the same fluid domain, so the velocity potential should be continuous at the radius of the cylinder. Using the Wronskian identity for Bessel functions, Evans and Porter (1997) combine the two boundary conditions

$$\int_b^h U_q^S(t) L_q(y,t)dt = \frac{-2i\alpha_{q,0}^S}{\pi ka J_q'(ka)}\psi_0(y), where L_q(y,t) \tag{36}$$

$$= -\sum_{i=1}^{\infty} \frac{\psi_i(y)\psi_i(t)}{k_i^2 ha I_q'(k_i a)K_q'(k_i a)}$$

The following equations in this subsection were derived by Evans and Porter (1997), and they are used as the numerical foundation of the computer program OWC Solution.

$$\alpha_{0,0}^{S} = \frac{-\pi kakhJ_1^2(ka)}{\pi kakhJ_1(ka)H_1(ka) + 2iS_{22}} \tag{37}$$

$$\alpha_{q,0}^{S} = \frac{-\pi kakhJ_q^{'}(ka)J_q^{'}(ka)}{\pi kakhJ_q^{'}(ka)H_q^{'}(ka) + 2iA_q^{S}} \tag{38}$$

The scattering induced volume flux across the free surface is

$$q^{S} = \frac{4\pi ikahJ_1(ka)S_{21}}{\pi kakhJ_1(ka)H_1(ka) + 2iS_{22}} \tag{39}$$

$S_{21}\ and\ S_{22}$ are the elements of the 2×2 matrix $\{S\}$, which can be calculated from

$$S \cong D^T L^{(0)^{-1}} D \tag{40}$$

In which $L^{(0)}$ is a $(N+1)\times(N+1)$ matrix, and D is a $(N+1)\times 2$ matrix

$$L_{mn}^{(0)} = \sum_{r=1}^{\infty} \frac{J_{2m}\{k_r(h-b)\}J_{2n}\{k_r(h-b)\}}{M_r^2 k_r hk_r aI_1(k_r a)K_1(k_r a)} \tag{41}$$

$$D_{1m} = \delta_{m0}\ , D_{2m} = (-1)^m \frac{1}{M_0} I_{2m}\{k(h-b)\} \tag{42}$$

And

$$A_q^{S} = \int_b^h u_q^{S} \cdot \psi_0 dy \cong F^T L^{(q)^{-1}} F \tag{43}$$

Where $F = (F_0, \dots, F_N)^T; F_m = (-1)^m \frac{1}{M_0} I_{2m}\{k(h-b)\}$

And

$$L_{mn}^{(q)} = -\sum_{r=1}^{\infty} \frac{J_{2m}\{k_r(h-b)\}J_{2n}\{k_r(h-b)\}}{M_r^2 k_r hk_r aI_q^{'}(k_r a)K_q^{'}(k_r a)} \tag{44}$$

This is the numerical method for us to calculate the hydrodynamic coefficients.

3.2 The free surface elevation comparison with experimental results

Experimental measurement of the free surface elevation can be used to verify the accuracy of the numerical model. An experiment was conducted in University of New Orleans by Garriga and Falzarano (2008). The free surface elevation in the experiment is measured at the center of the cylinder (r=0). Using the computer program OWC Solution, we can calculate the water surface elevation at the center of the cylinder and compare it with the experiment results.

If we define the incident wave height as H_{inc}, then the incident wave potential in cylindrical

coordinates is

$$\Phi_{inc} = Re\{\sum_{q=0}^{\infty} \epsilon_q \, i^q J_q(kr)\cos(q\theta)\psi_0(y)\, e^{-i\omega t}\} \cdot \frac{H_{inc}}{2} \cdot \frac{g}{w} \cdot \frac{1}{\psi_0(y)\big|_{y=0}} i \tag{45}$$

Since we are using linear wave theory, when we multiply the incident wave potential $\phi^I e^{-iwt}$ with $\frac{H_{inc}}{2} \cdot \frac{g}{w} \cdot \frac{1}{\psi_0(y)\big|_{y=0}} i$, we will get the wave potential when the incident wave height is H_{inc}.

So the wave potential inside the cylinder is

$$\Phi_{OWC} = Re\{\phi^S \cdot e^{-iwt} \cdot \frac{H_{inc}}{2} \cdot \frac{g}{w} \cdot \frac{1}{\psi_0(y)\big|_{y=0}} i\} \tag{46}$$

If we define the wave height at the center of the cylinder as H_{OWC}

$$H_{OWC} = Re\{\sum_{q=0}^{\infty} \epsilon_q \, i^q \cos(q\theta)\left[\beta_{q,0}^S J_q(kr)\psi_0(y) + \sum_{i=1}^{\infty} \beta_{q,i}^S \, I_q(k_i r)\psi_i(y)\right] e^{-i\omega t}\} \cdot \frac{H_{inc}}{2} \tag{47}$$

H_{OWC} and H_{inc} are defined as real numbers. The Visual Basic program OWC Solution can solve for the hydrodynamic coefficients $\beta_{q,0}^S$ corresponding to the qth order of the expansion, and then we can calculate the wave height at any point inside the cylinder.

A series of OWC experiments were conducted by Garriga and Falzarano (2008) in the University of New Orleans towing tank (38.100 m long, 4.572 m wide and 1.929 m deep for this model test). The OWC model with opened top was mounted at the towing tank's carriage 13.716 m away from the wave maker.

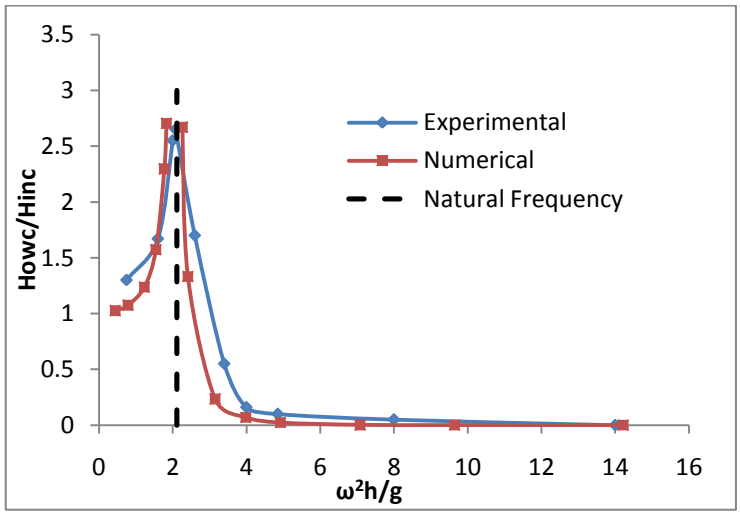

Fig. 2 Comparison between experimental and numerical result (b=0.762 m)

The parameters used by Garriga and Falzarano (2008) in the UNO model test are: the radius a=0.305 m; the draft b=0.762 m; the water depth h= 1.929 m; the incident wave frequency ω is varied. Fig. 2 is the plot of the comparison between experimental and numerical result when b=0.762 m.

Fig. 3 is the plot of the comparison between experimental and numerical result when b=0.509 m.

The parameters used by Garriga and Falzarano (2008) in the UNO model test are: the radius a=0.305 m; the draft b=0.509 m; the water depth h= 1.929 m; the incident wave frequency ω is varied.

The fact that experimental results are larger than the numerical results except in the narrow region of resonance is possibly caused by the reflected wave in the model test or side wall effects.

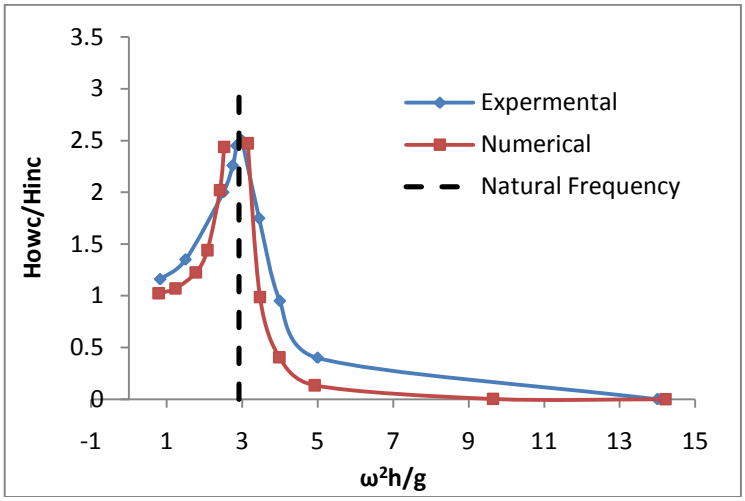

Fig. 3 Comparison between experimental and numerical result (b=0.509 m)

3.3 The natural frequency approximation

Faltinsen (1990) gave the natural frequency equation of a moon pool: $\omega_n = \sqrt{\frac{g}{b}}$, which is an approximation of the heave natural frequency of a floating walled body ignoring the effect of added mass.

According to Karami *et al*. (2012), we can generally write the equation of motion for the oscillating water column as

$$(m + m_a)\frac{d^2\eta}{dt^2} + (B_r + B_a)\frac{d\eta}{dt} + K_r\eta = F_S \tag{48}$$

Where m is the mass of water column inside the cylinder at its equilibrium, m_a is the added mass of water column in the heave direction, B_r is the radiation damping coefficient, B_a is the applied damping coefficients, K_r is hydrostatic stiffness, and F_S is the exciting force due to the scattering (incident and diffraction) potential. The viscous damping is not considered in this model.

Considering the added mass of the oscillating water column by Falnes (2002), an amendment to

Faltinsen's (1990) approximation for the natural frequency is given

$$\omega_n = \sqrt{\frac{\rho g \pi a^2}{\rho \pi a^2 b + 0.5\pi\rho a^3}} = \sqrt{\frac{g}{b + 0.5a}} \tag{49}$$

In which $\rho g \pi a^2$ represents the hydrostatic stiffness of the OWC system because of the restoring force resultant of gravity and buoyancy. $F_R = -\rho g \pi a^2 \eta$, η is the internal wave elevation. $\rho \pi a^2 b$ is the mass of water column inside the cylinder at its equilibrium position in vertical direction; $0.5\pi\rho a^3$ is the approximation for added mass of the water column; πa^2 is the water plane area inside the cylinder.

Fig. 4 is the wave height transfer function when you fix different geometric parameters, we can use the above natural frequency equation to estimate the natural frequency.

When the cylinder radius a=0.914 m, the draft b=1.524 m, water depth h= 6.096 m and the incident wave height H_{inc}=0.213 m, we can find that the natural frequency $\omega_n = 2.22\, rad/s$, and the nondimensional natural frequency is 3.077, which matches the numerical result.

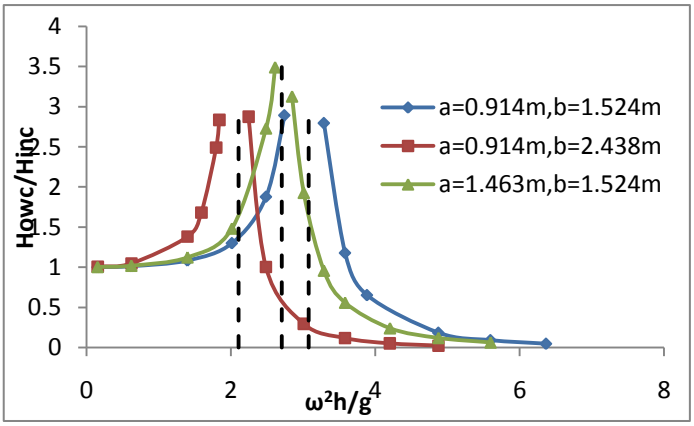

Fig. 4 Wave height ratio for different geometry of the OWC

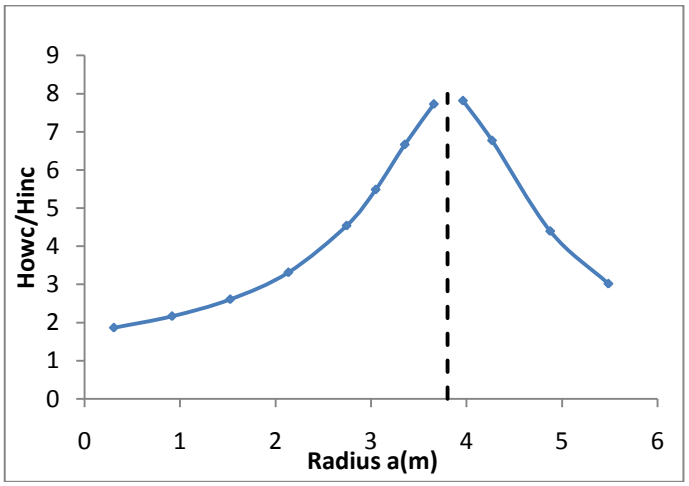

Fig. 5 Wave height transfer ratio with the radius of the cylinder

When the radius a=0.914 m, the draft b=2.438 m, the water depth h= 6.096 m and the incident wave height H_{inc}=0.213 m, we can find that the natural frequency $\omega_n = 1.84\, rad/s$, and the nondimensional natural frequency is 2.105, which matches numerical result.

When the radius a=1.463 m, the draft b=1.524 m, the water depth h= 6.096 m and the incident wave height H_{inc}=0.213 m, we can find that the natural frequency $\omega_n = 2.085\, rad/s$,and the nondimensional natural frequency $\omega_n{}^2 h/g$ is 2.703, which matches numerical result.

The nondimensional natural frequencies calculated by Eq. (34) for the first experiment is 2.11, and 2.92 for the second experiment, which match the experiment curves very well.

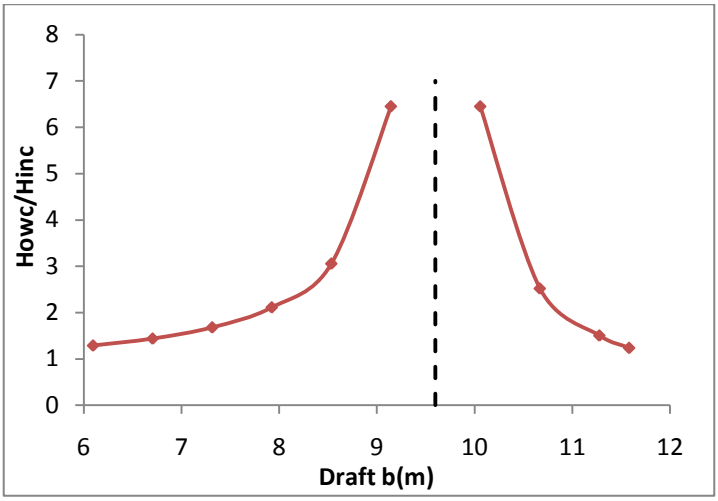

Fig. 6 Wave height transfer ratio with the draft of the cylinder

3.4 Geometric parameters effect on the response amplitude operator

The following calculations show us how the response inside the cylinder is affected by varying certain geometric parameter, when you fix the other parameters.

Initial value: a= 0.305 m; b=7.62 m; h=15.24 m; ω= 1 rad/s. We change only the radius of the cylinder to see how the radius affects the wave amplitude inside the cylinder. The results are shown in Fig. 5. We can observe that the RAO reaches peak when a=3.8 m, $\omega_n = \sqrt{\frac{9.81}{7.62+3.8/2}}$ =1.015 rad/s, which is very close to the incident wave frequency.

Then we change only the draft of the cylinder to see how the draft affects the response inside the cylinder. The results are shown in Figure 6.It can be observed that the RAO reaches peak when b=9.6 m, estimated $\omega_n = 1.006\, rad/s$, which is very close to the incident wave frequency (1 rad/s).

We change only the water depth to see how the water depth affects the response inside the cylinder. The results are shown in Fig. 7:

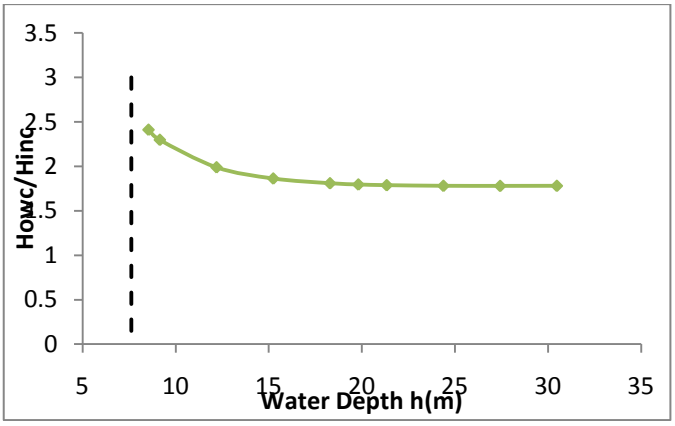

Fig. 7 Wave height transfer ratio with respect to the water depth

The draft of the cylinder b=7.62 m acts like a "wall" to the RAO curve. The RAO over the water depth indicates the bottom effect of the system: when the draft of the cylinder becomes close to the water depth, the response inside the cylinder will be significantly affected by the bottom.

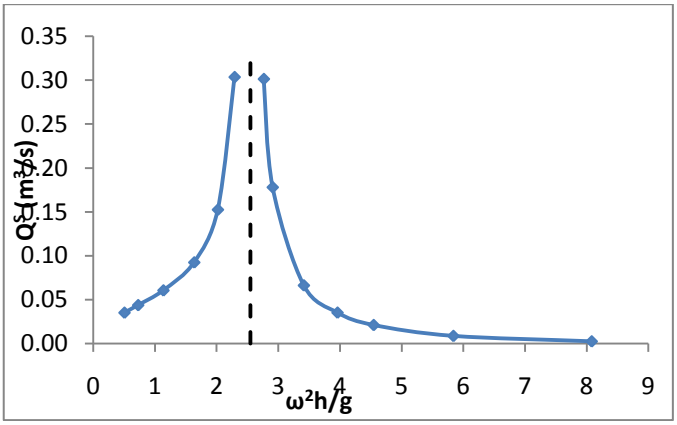

Fig. 8 Scattering induced volume flux with respect to frequency

3.5 Scattering volume flux inside the cylinder

Fig. 8 shows the scattering volume flux with respect to the incident wave frequency. Set a= 0.305 m; b=7.62 m; h=19.812 m; we only change the incident wave frequency:

Using the natural frequency equation $\omega_n = 1.123$ rad/s; $\omega_n{}^2 h/g = 2.549$. We can observe that the volume fluxes have large values near the natural frequency and it has a similar curve with the H_{OWC}/H_{inc} curve.

3.6 Fluid motion inside the cylinder

The fluid motion inside the cylinder is not uniform across the water plane inside the cylinder. If we set the radius a=0.610 m; the draft b=3.048 m; the water depth h= 12.192 m; the incident wave frequency ω=1 rad/s; the incident wave height H_{inc}=0.213 m. Fig, 9 shows the wave height with respect to axial coordinate:

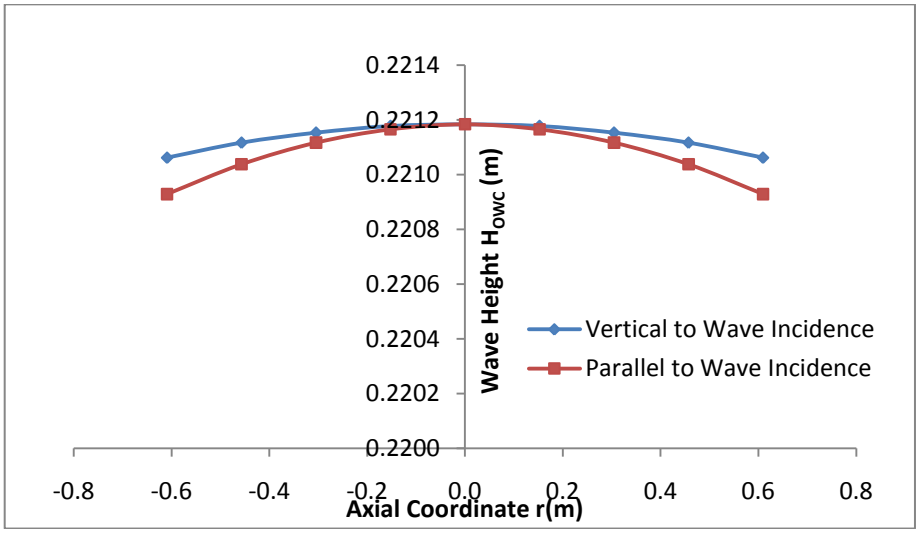

Fig. 9 Wave height profile across the horizontal plane inside the cylinder

We can note that the wave height at different points inside the cylinder is quite close (0.12% difference). The center of the cylinder has the highest wave height and the wave height decreases as it comes closer to the radius of the cylinder.

3.7 The radiation problem by oscillating chamber pressure

The radiation problem is concerned with the fluid motion when there is no incident wave, but oscillating air pressure exists on the water column inside the cylinder.

The solution for the radiation problem in this subsection was derived by Evans and Porter (1997). Corresponding to air pressure oscillation amplitude p, outside the cylinder:

$$\phi^R = \begin{cases} \alpha_0^R H_0(kr)\psi_0(y) + \sum_{n=1}^{\infty} \alpha_n^R K_0(k_n r)\psi_n(y)\,, \text{outside the cylinder} \\ \beta_0^R J_0(kr)\psi_0(y) + \sum_{n=1}^{\infty} \beta_n^R I_0(k_n r)\psi_n(y) + \frac{g}{\omega^2}\,, \text{inside the cylinder} \end{cases} \tag{50}$$

α_0^R and β_0^R are the coefficients for the radiation wave potential, where α_n^R and β_n^R are coefficients for higher order terms.

Based on continuity of the radial velocity at the radius of the cylinder, we can achieve the relationship between the hydrodynamic coefficients for the potential inside and outside the

cylinder.

In addition, the fluid potential is continuous at the radius of the cylinder. So we can get another equation between the coefficients of wave potential inside and outside the cylinder

According to the result given by the Galerkin approximation in subsection 3.1

$$\alpha_0^R = \frac{\frac{g}{\omega^2}\pi k a J_1(ka) S_{12}}{\pi k a k h J_1(ka) H_1(ka) + 2iS_{22}} \tag{51}$$

$$q^R = \frac{2\pi\frac{g}{\omega^2} a[\pi k a k h J_1(ka) H_1(ka) S_{11} + 2i(S_{11}S_{22} - S_{12}S_{21})]}{\pi k a k h J_1(ka) H_1(ka) + 2iS_{22}} \tag{52}$$

The following is the radiation volume flux in the frequency domain, as shown in Fig. 10. Set p=968.325 Pa; a=0.610 m; b=7.62 m; h=19.812 m:

The radiated waves have the same natural frequency as the scattered waves for a given cylinder, which can be calculated by: $\omega_n = 1.112$ rad/s; ${\omega_n}^2 h/g$=2.500.

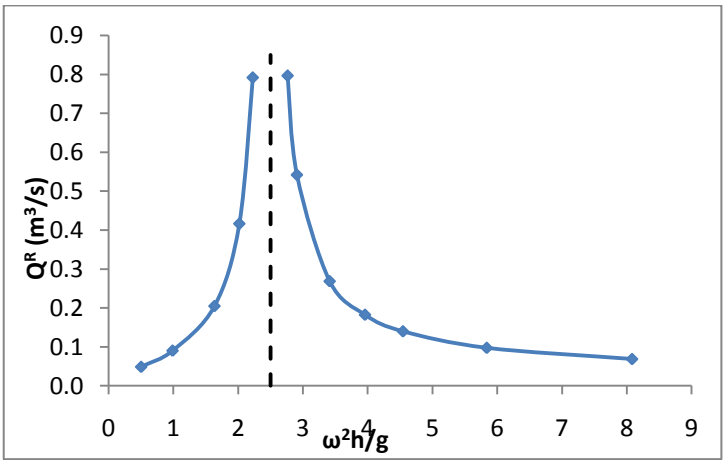

Fig. 10 Radiation volume flux with respect to frequency

4. Wave energy analysis from an OWC device

4.1 Model of air flow and air compression for the OWC system

The idea of the OWC device is extracting wave energy to generate electricity through an air turbine at the top of the cylinder. This involves the interaction between the air motion (determined by the air turbine, volume of the air chamber above the water surface and air compressibility) and water motion (determined by the incident wave and geometric parameters of the truncated vertical cylinder). The derivations in this subsection are given according to the derivations by Malmo and Reitan (1985) for an oscillating water column with square geometry.

We can define the water volume under the free surface inside the cylinder as V_η. If we denote the air volume through the turbine by V_t, and denote the air volume inside the cylinder at certain

pressure by V_p

$$\frac{dV_\eta}{dt} - \frac{dV_t}{dt} = -\frac{dV_p}{dt} \tag{53}$$

The water volume flux is decomposed into two parts by Evans and Porter (1995)

$$\frac{dV_\eta}{dt} = q^S - \frac{i\omega p}{\rho g} q^R \tag{54}$$

q^S is the scattering volume flux across the horizontal plane inside the cylinder; $\frac{iwp}{\rho g} q^R$ is the radiation volume flux across the horizontal plane inside the cylinder. The air flow rate through the turbine is

$$\frac{dV_t}{dt} = C_t \cdot p_e \tag{55}$$

This is a linearity assumption that the air flow rate through the turbine is proportional to the air pressure and turbine constant, which was suggested by Malmo and Reitan (1985). C_t is the turbine constant; which is a ratio between the air flow and the pressure drop through the turbine.

Since the incident wave is time harmonic, $q^S \; and \; q^R$ are also time harmonic, Q^S and Q^R is the complex magnitude of each variable. . For given amount of air

$$P \cdot {V_p}^\gamma = Constant \tag{56}$$

If we assume this to be an adiabatic process, then γ=1.4.

Two linearity assumptions are made here, which are suggested by Malmo and Reitan (1985):

(1)$P(t) = p_a + p_e$, fluctuating air pressure p_e is very small compared with the atmosphere air pressure p_a;

(2) $V_p = V_C + V_e(t)$, fluctuating air chamber volume V_e is small compared with the original air chamber volume V_C.

So

$$dV_p = -\frac{V_C dp_e}{\gamma p_a} \tag{57}$$

After removing the time dependence, we can combine all the terms in the following equation

$$Q^S - \frac{i\omega p}{\rho g} Q^R = C_t \cdot p + \frac{V_C}{\gamma p_a} \cdot p \cdot (-i\omega) \tag{58}$$

According to linearity, the scattering volume flux corresponding to incident wave with wave height H_{inc} is

$$Q^S = \frac{4\pi ikahJ_1(ka)S_{21}}{\pi kakhJ_1(ka)H_1(ka) + 2iS_{22}} \cdot \frac{H_{inc}}{2} \cdot \frac{g}{w} \cdot \frac{1}{\psi_0(y)\Big|_{y=0}} i \tag{59}$$

This is the equation that relates the hydrodynamics problem of open-top OWC to the air flow from a turbine-connected OWC system. There will be an air pressure fluctuation above the water surface in the turbine-connected air chamber, which causes the wave radiation. This equation can be used to solve for oscillating air pressure and air flow through the turbine. Note that p, C_t, Q^S and Q^R is the complex magnitudes, so phases are also important in the air-water interaction.

4.2 Energy analysis

The energy input into this system is provided by the incident wave. According to Dean and Dalrymple (1984), the energy input rate is

$$P_i = \left(\frac{1}{8}\rho g {H_{inc}}^2\right)\frac{\omega}{k}\left[\frac{1}{2}\left(1+\frac{2kh}{sinh(2kh)}\right)\right]\cdot(2a) \tag{60}$$

In which

$$C_g = \frac{\omega}{k}\left[\frac{1}{2}\left(1+\frac{2kh}{sinh(2kh)}\right)\right] \tag{61}$$

C_g is the group velocity for the wave energy transmitting, and a is the radius of the cylinder. The air flow power driving the turbine is

$$P_t = \frac{1}{T}\int_0^T Re\{[Re(p)+iIm(p)]e^{-i\omega t}\}Re\{[Re(Q_t)+iIm(Q_t)]e^{-i\omega t}\}dt \tag{62}$$

T is the period of the incident wave. So

$$P_t = \frac{1}{2}[Re(p)Re(Q_t)+Im(p)Im(Q_t)] \tag{63}$$

4.3 Turbine constant effect on the OWC system

The following is a study considering the energy output with respect to the turbine constant (real part). Set the radius a=2.438 m; and the draft b=7.62 m; for a water depth h= 24.384 m; and incident wave height H_{inc}=0.914 m. The incident wave frequency $\omega = 1\,rad/s$, the air chamber volume V_C=339.802 m^3. Usually the real part of the turbine is much larger than the imaginary part of the turbine constant, indicating that the change of air flow is basically in phase with the pressure drop. When we set the imaginary part of the turbine to be 0, the effect of real part of the turbine constant is shown in Figs. 11 and 12:

We can find in Figs. 11 and 12 that the pressure variation inside the cylinder is decreasing with the increase of the turbine constant; while the air flow inside/outside the cylinder is growing with the increase of the turbine constant, and it converges to the scattering volume flux Q^S, which is reasonable because when the turbine constant goes to infinity, there will not be a turbine. $Q^S = 39.147\ \mathrm{m}^3/s$ in these cases. Fig. 13 shows how the energy is distributed in the system

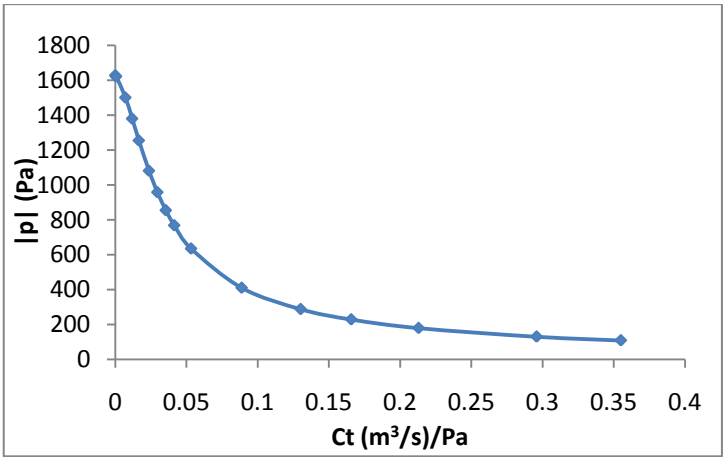

Fig. 11 Pressure variation magnitude with turbine constant real part

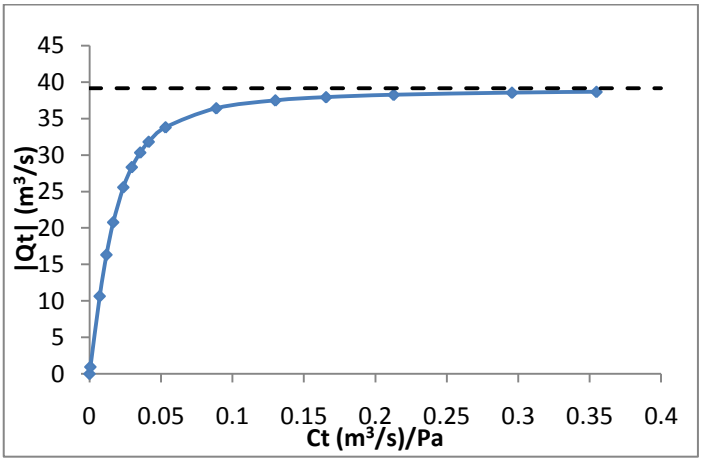

Fig. 12 Air flow rate with turbine constant real part

The imaginary part of turbine constant will lead to a phase lag, which means the peak of flow rate occurs at a different phase from the pressure variation peak, and this is not negligible for large scale turbines.

A study about the effect of the imaginary part of turbine constant is done below. Set the radius a=1.219 m; the draft b=3.048 m; the water depth h= 18.288 m; the incident wave frequency ω=1.5 rad/s; the incident wave height H_{inc}=0.610 m; the air chamber volume V_C=56.634 m^3.

If we assume no phase lag (zero imaginary part for the turbine constant), the optimal energy solution is shown in Table 1:

Table 1 Optimal solution with zero imaginary part

C_t	Real	Imaginary
$(m^3/s)/(Pa)$	5.30E-03	0.0000
Theoretical	3735.46	Watt
Output	1442.23	Watt
Efficiency	38.61%	
H_{OWC}/H_{inc}	2.236	

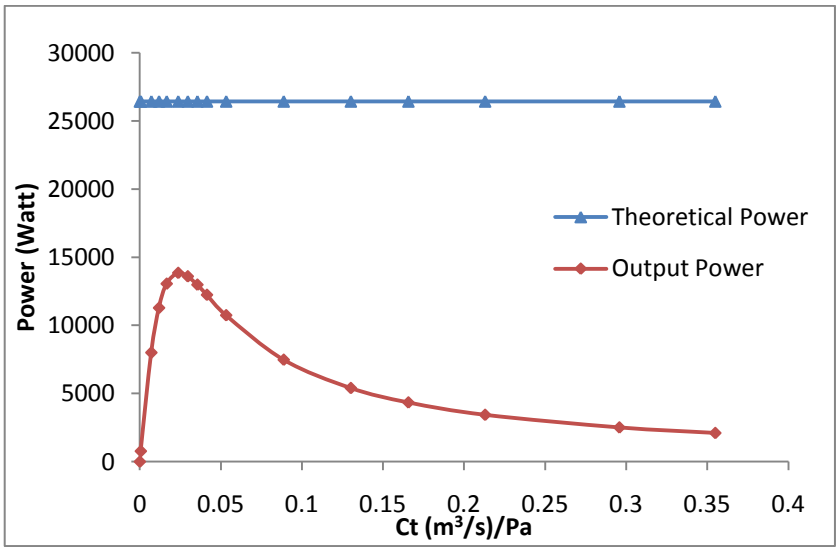

Fig. 12 Energy analysis with respect to turbine constant real part

The real turbine constant has a mathematical optimal value given by Cho (2002)

$$C_t = \sqrt{\left[Re\left(\frac{\omega}{\rho g} Q^R\right)\right]^2 + [Im(\frac{\omega}{\rho g} Q^R) + \frac{V_C \omega}{\gamma p_a}]^2} \tag{64}$$

The mathematical optimal value is 0.0053 $(m^3/s)/(Pa)$, which matches the program. When imaginary part of turbine constant is limited to 10% of the real part, that is, a maximum 5.71° phase lag of the turbine is allowed, the energy solution is shown in Table 2.

It can be found from the cases above that the phase lag helps to increase the efficiency of the system. According to Falnes (2002), the imaginary part of the turbine constant can be important for a large scale OWC, but it is usually negligible in small scale OWC (typically used in laboratory experiments). Future data about the turbine constant for a real turbine can be applied to get a more realistic result.

Table 2 Solution with a 10% imaginary part

Ct	Real	Imaginary
$(m^3/s)/(Pa)$	5.27E-03	5.27E-04
Theoretical	3735.46	Watt
Output	1575.01	Watt
Efficiency	42.16%	
H_{OWC}/H_{inc}	2.236	

4.4 Discussion about the turbine

In this subsection, the authors will discuss the availability of the turbine with our desired turbine constant. The Wells turbine is often used in OWC system to extract the wave energy. Gato and Falcão (1988) have studied the aerodynamics of the Wells turbine using a numerical model. However, it is easier to find the performance of a Wells turbine in a given OWC system if we have the experiment data of a Wells turbine. Camporeale *et al*. (2011) have provided the experiment performance data of a Wells turbine.

As an example, consider the case of the cylinder tested in the UNO towing tank by Garriga and Falzarano (2008). The radius of the cylinder a= 0.305 m; the draft of the cylinder b=0.762 m; the water depth h= 1.929 m; set the incident wave height H_{inc}= 0.305 m; the incident wave frequency ω= 3 rad/s (this is close to the natural frequency which results in the largest scatter volume flux inside the cylinder) and the volume of air chamber to be V_C= 1.982 m^3. This is a small scale case that will be used in order to illustrate the optimal selection of an air turbine.

Since this is a small scale case, the imaginary part of the turbine constant is typically negligible.

The scattered volume flux Q^S is given by Eq. (59), radiation volume flux Q^R is given by Eq. (52),air flow through the turbine $C_t \cdot p$ can be calculated by Eq. (58).The authors run the Visual Basic program OWC Solution through different values for the air turbine constant, and find the optimal turbine constant with maximum energy output from the turbine.

The maximum energy output is when the turbine constant is $6.275 \times 10^{-4}$$(m^3/s)/Pa$, which matches Eq. (64) by Cho with predicted optimal *Ct* value to be 6.277×10^{-4} $(m^3/s)/Pa$. The wave height RAO H_{OWC}/H_{inc} =2.298; the pressure variation is 412.774 Pa; air flow magnitude through the turbine is 0.259 m^3/s; the output energy is 53.48 Watts with a 40.87% transfer efficiency from the incident wave power.

This design can be realized with a small scale Wells turbine similar to that already built and tested by Camporeale *et al*. (2011). They used the following nondimensional values in their experiments on the Wells turbine performance in an oscillating flow

$$p' = \frac{p}{\rho_a {\omega_t}^2 {R_{tip}}^2} \tag{65}$$

$$v' = \frac{Q_t}{\pi({R_{tip}}^2 - {R_{hub}}^2)\omega_t R_{tip}} \tag{66}$$

In which p' and v' is the pressure drop and average axial velocity in nondimensional form, ρ_a=1.2922 kg/m^3 is the density of air at 0°C, ω_t is the angular rotation speed of the turbine. Experiments by Camporeale et al. (2011) provided the pressure drop (p') curve versus average axial velocity (v') for a Wells turbine with a hub radius R_{hub}=101 mm, a tip radius R_{tip}= 155 mm, a blade chord 74 mm, 7 constant chord blades and a NACA0015 blade profile.

The rotational speed ω_t can be changed by adjusting the turbine constant of this existing turbine to meet our design requirements as shown in Table 3.

Table 3 Select rotational speed for the turbine

N (rpm)	ω_t (rad/s)
1241.41	130
v'	p'
0.296	0.787

According to Eqs. (65) and (66), when the average axial velocity v'=0.296; the pressure drop p' ≅ 0.75, according to experiments by Camporeale *et al*. (2011). So when we dimensionalize the pressure drop and air flow rate for the actual turbine used in their experiment, the air flow magnitude through the turbine is 0.259 m^3/s, and the pressure drop is 393.5Pa, having only 4.9% difference form our design. The rotational speed of 1241.41 rpm is a reasonable rotational speed for the Wells turbine that Camporeale *et al*. (2011) have tested.

It can be found from the case above that the existing air turbine can be used to realize our design for the OWC system if we have the experimental data of pressure drop versus axial air flow velocity, which is a typical test for an air turbine.

5. Conclusions

The numerical results of the free surface elevation inside the cylinder agree reasonably well with the experimental results given by Garriga and Falzarano (2008) obtained in the UNO towing tank. The ratio between the wave height at the center of cylinder and the incident wave height has a typical transfer function shape with obviously different values only at a small frequency range near the natural frequency.

The geometric parameters of the cylinder (radius and draft) determine the natural frequency and the wave height transfer function, in which draft has a more significant effect. Water depth will also influence the flow field with the bottom effect obviously when draft comes close to water depth. Wave radiation from the OWC system also shows a similar transfer function with peak values at the same natural frequency decided by geometric parameters.

The extended study on the energy output from the OWC system indicates that the air turbine constant is very important to extract energy from the incident waves. The possible phase lag (between air flow and pressure drop) that an air turbine can reach is very important to the OWC efficiency.

Acknowledgements

The instructions to this research from Prof. Jeffrey Falzarano are highly acknowledged. The authors wish to acknowledge the experiment results from University of New Orleans provided by Mr. Octavi Garriga and Prof. Jeffrey Falzarano. Prof. Moo-Hyun Kim from Texas A&M University Ocean engineering program, Professor Alan Palazzolo from Texas A&M University mechanical engineering department and Dr. Neil Brown from NAB Associates, Inc. also provided very helpful advices for this research.

References

Abramowizt, M.A. and Stegun, I. (1964), *Handbook of Mathematical Functions*, Dover Publications, New York, NY, USA.

Camporeale, S.M., Filianoti, P. and Torresi, M. (2011), "Performance of a Wells turbine in an OWC device in comparison to laboratory tests", *Proceedings of the 9th European Wave and Tidal Energy Conference*, Southampton, UK.

Chakrabarti, S.K. (1987), *Hydrodynamics of offshore structures*. WIT Press, Southampton, UK.

Cho, I.H. (2002), "Wave energy absorption by a circular oscillating water column device", *J. Korean Soc. Coast. Ocean Engineers*, **14**(1), 8-18.

Dean, R.G. and Dalrymple, R.A. (1984), *Water wave mechanics for engineers and scientists*, World Scientific Publishing, Singapore.

Evans, D.V. (1982), "Wave-power absorption by systems of oscillating surface pressure distributions", *J. Fluid Mech.*, **114**, 481-499.

Evans, D.V. and Porter, R. (1995), "Hydrodynamic characteristics of an oscillating water column device", *Appl. Ocean Res.*, **17**, 155-164.

Evans, D.V. and Porter, R. (1997), "Efficient calculation of hydrodynamic properties of OWC-type devices", *J. Offshore Mech. Arct.*, **119**, 210-218.

Falnes, F. (2002), *Ocean waves and oscillating systems*, Cambridge University Press, Cambridge, UK.

Faltinsen, O.M. (1990), *Sea loads on ships and offshore structures*, Cambridge University Press, Cambridge, UK.

Brennan, F.P., Falzarano, J.M., Gao, Z., Landet, E., Boulluec, M.L., Rim, C.W., Sirkar, J., Sun, L., Suzuki, H., Thiry, A., Trarieux, F. and Wang, C.M. (2012), "Offshore renewable energy", *Proceedings of the 18th International Ship and Offshore Structures Congress*, Rostock, Germany.

Garrett, C.J.R. (1970), "Bottomless harbours", *J. Fluid Mech.*, **43**(3), 433-449.

Garriga, O.S. and Falzarano, J.M. (2008), "Water wave interaction on a truncated vertical cylinder", *J. Offshore Mech. Arct.*, **130**, 031002(1-8).

Garriga, O.S. (2003), *Water waves and marine structure interaction*, Master's thesis, University of New Orleans, New Orleans.

Gato, L. and Falcão, A.F. de O. (1988), "Aerodynamics of the wells turbine", *Int. J. Mech. Sci*., **30**(6), 383-395.

Haberman, R. (2004), *Applied partial differential equations with fourier series and boundary value problems*, Pearson Education, Upper Saddle River, NJ.

Karami, V., Ketabdari, M.J. and Akhtari, A.K. (2012), "Numerical modeling of oscillating water column wave energy convertor", *Int. J. Adv. Renew. Energy Res.*., **1**(4), 196-206.

Koo, W. and Kim, M.H. (2010), "Nonlinear time-domain simulation of a land-based oscillating water column", *J. Waterw. Port C. - ASCE*, **136**(5), 276–285.

Koo, W.C. and Kim, M.H. (2012), "A time-domain simulation of an OWC (Oscillating Water Column) with irregular waves", *Ocean Syst. Eng.*, **2**(2), 147-158.

Linton, C.M. and Evans, D.V. (1992), "The radiation and scattering of surface waves by a vertical circular cylinder in a channel", *Philos. T. R. Soc. Lond. A.*, **338**, 325-357.

Malmo, O. and Reitan, A. (1985), "Wave-power absorption by an oscillating water column in a channel", *J. Fluid Mech.*, **158**, 153-175.

Sarmento, A.J.N.A. and Falcão, A.F. de O. (1985), "Wave generation by an oscillating surface pressure and its application in wave-energy extraction", *J. Fluid Mech.*, **150**, 467-485.

Wang, H. (2013), *Wave energy extraction from an oscillating water column in a truncated circular cylinder*, Master Thesis, Texas A&M University.